

ACCELERATED COMMUNICATION

Prostaglandin-Induced Activation of Nociceptive Neurons via Direct Interaction with Transient Receptor Potential A1 (TRPA1)

Thomas E. Taylor-Clark, Bradley J. Udem, Donald W. MacGlashan, Jr., Srinivas Ghatta, Michael J. Carr, and M. Allen McAlexander

Johns Hopkins University, Department of Medicine, Baltimore, Maryland (T.E.T.-C., B.J.U., D.W.M.); GlaxoSmithKline Pharmaceuticals, Respiratory and Inflammation Centre of Excellence for Drug Discovery, Target Discovery, King of Prussia, Pennsylvania (S.G., M.J.C., M.A.M.)

Received August 10, 2007; accepted November 13, 2007

ABSTRACT

Inflammation contributes to pain hypersensitivity through multiple mechanisms. Among the most well characterized of these is the sensitization of primary nociceptive neurons by arachidonic acid metabolites such as prostaglandins through G protein-coupled receptors. However, in light of the recent discovery that the nociceptor-specific ion channel transient receptor potential A1 (TRPA1) can be activated by exogenous electrophilic irritants through direct covalent modification, we reasoned that electrophilic carbon-containing A- and J-series prostaglandins, metabolites of prostaglandins (PG) E₂ and D₂, respectively, would excite nociceptive neurons through direct activation of TRPA1. Consistent with this prediction, the PGD₂ metabolite 15-deoxy-Δ^{12,14}-prostaglandin J₂ (15dPGJ₂) activated heterologously expressed human TRPA1 (hTRPA1-HEK), as well as a subset of chemosensitive mouse trigeminal neurons. The effects of 15dPGJ₂ on neurons were blocked by both the nonselective TRP channel blocker

ruthenium red and the TRPA1 inhibitor (HC-030031), but unaffected by the TRPV1 blocker iodo-resiniferatoxin. In whole-cell patch-clamp studies on hTRPA1-HEK cells, 15dPGJ₂ evoked currents similar to equimolar allyl isothiocyanate (AITC) in the nominal absence of calcium, suggesting a direct mechanism of activation. Consistent with the hypothesis that TRPA1 activation required reactive electrophilic moieties, A- and J-series prostaglandins, and the isoprostane 8-iso-prostaglandin A₂-evoked calcium influx in hTRPA1-HEK cells with similar potency and efficacy. It is noteworthy that this effect was not mimicked by their nonelectrophilic precursors, PGE₂ and PGD₂, or PGB₂, which differs from PGA₂ only in that its electrophilic carbon is rendered unreactive through steric hindrance. Taken together, these data suggest a novel mechanism through which reactive prostanoids may activate nociceptive neurons independent of prostaglandin receptors.

Peripheral inflammation induces the formation of prostaglandins (PGs), both centrally and peripherally, which contribute to pain sensation and sensitivity (Woolf and Costigan, 1999; Burian and Geisslinger, 2005). During inflammation, a superfamily of phospholipase A₂ enzymes hydrolyzes membrane phospholipids to release arachidonic acid, which is subsequently converted by cyclooxygenases (COXs) into

PGH₂. Through the actions of tissue-specific isomerases, a variety of prostaglandins is formed from this intermediate; for example, PGE₂, PGD₂, and PGI₂. The contribution of prostaglandins to inflammatory pain is extensively documented and is demonstrated by the analgesic properties of COX inhibitors (Burian and Geisslinger, 2005). Research has followed into the specific mechanisms and pathways through which prostaglandins contribute to inflammation and nociception and many prostaglandin receptors (including those for PGE₂, PGD₂, and PGI₂) have been demonstrated on sensory nerves (Jenkins et al., 2001; Moriyama et al., 2005).

The nonselective cation channel transient receptor poten-

This work was supported by the National Institutes of Health and GlaxoSmithKline.

Article, publication date, and citation information can be found at <http://molpharm.aspetjournals.org>.
doi:10.1124/mol.107.040832.

ABBREVIATIONS: PG, prostaglandin; COX, cyclooxygenase; AITC, allyl isothiocyanate; FBS, fetal bovine serum; 15dPGJ₂, 15-deoxy-Δ^{12,14}-prostaglandin J₂; I-RTX, iodo-resiniferatoxin; RR, Ruthenium red; HC-030031, 1,2,3,6-tetrahydro-1,3-dimethyl-N-[4-(1-methylethyl)phenyl]-2,6;-NS398, N-[2-(cyclohexyloxy)-4-nitrophenyl]-methane sulfonamide; hTRPA1-HEK, human embryonic kidney 293 cells stably transfected with human TRPA1 channels; nt-HEK, nontransfected human embryonic kidney 293 cells.

tial (TRP) A1 is primarily expressed in small diameter, nociceptive neurons (Story et al., 2003; Katsura et al., 2006; Hjerling-Leffler et al., 2007), where its activation probably contributes to the perception of noxious stimuli and inflammatory hyperalgesia (Bautista et al., 2006; Kwan et al., 2006; McNamara et al., 2007). Multiple mechanisms converge to regulate TRPA1's function, because it can be activated by inflammatory mediators through G_q/phospholipase C pathways (Bandell et al., 2004; Jordt et al., 2004), by intracellular calcium directly (Doerner et al., 2007; Zurborg et al., 2007), and by plant-derived compounds such as carvacrol (Xu et al., 2006) and Δ⁹-tetrahydrocannabinol (Jordt et al., 2004). In addition, recent studies have described a novel mechanism through which allyl isothiocyanate (AITC) and other electrophilic irritants can activate TRPA1 by covalently binding to cysteine residues within the cytosolic N terminus of the channel (Hinman et al., 2006; Macpherson et al., 2007).

Inflammation can lead to the formation of electrophilic compounds in vivo (Stamatakis and Perez-Sala, 2006). In particular, cyclopentenone ring-containing A- and J-series prostanoids are formed as nonenzymatic dehydration products of PGE₂ and PGD₂, respectively (Fitzpatrick and Waynald, 1981; Herlong and Scott, 2006). Although these molecules have been studied because of their effects on cell growth, cytokine production, chemotaxis, and cytotoxicity (Gayarre et al., 2006; Herlong and Scott, 2006), their role in nociception remains largely unexplored. We hypothesize here that certain prostanoids may participate in nociception independently of prostaglandin receptors. In particular, we address the hypothesis that prostanoids containing electrophilic moieties may stimulate nociceptive sensory nerves via direct activation of TRPA1, suggesting a novel mechanism through which inflammation stimulates nociceptive pathways.

Materials and Methods

Dissociation of Mouse Trigeminal Neurons. The methods were modified from those described previously (Taylor-Clark et al., 2005). All experiments were approved by the Johns Hopkins Animal Care and Use Committee. In brief, male C57BL6 mice (20–40 g) were euthanized by CO₂ overdose, and the trigeminal ganglia were rapidly dissected and cleared of adhering connective tissue. The medial portion of the ganglia was isolated (contains neurons that innervate the upper airways) and incubated in 2 mg/ml collagenase type 1A and 2 mg/ml dispase II in 2 ml of Ca²⁺-free, Mg²⁺-free HBSS (18 h, 4°C; then 10 min, 37°C). Neurons were dissociated by trituration, washed by centrifugation, resuspended in L-15 medium containing 10% FBS and then transferred onto circular 25-mm glass coverslips (Bellco Glass Inc., Vineland, NJ) coated with poly-D-lysine (0.1 mg/ml) and laminin (5 μg/ml, 25 μl per coverslip). Coverslips were used within 24 h.

HEK293 Cell Culture. In addition to wild-type HEK293 cells, cells stably expressing human TRPA1 [hTRPA1-HEK (Hill and Schaefer, 2007)] or human TRPV1 [hTRPV1-HEK (Hayes et al., 2000)] were used in the current study. Cells were maintained in an incubator (37°C, 5% CO₂) in Dulbecco's modified Eagle's medium (containing 110 mg/l pyruvate) supplemented with 10% FBS and 500 μg/ml G-418 (Geneticin) as a selection agent. Cells were removed from their culture flasks by treatment with Accutase (Sigma, St. Louis, MO), then plated onto poly-lysine-coated cover slips (BD Biosciences, Bedford, MA) and incubated at 37°C for >1 h before experimentation.

Calcium Imaging. HEK293-covered coverslips were loaded with Fura 2 acetoxyethyl ester (Fura-2 AM; 8 μM) (Molecular Probes,

Carlsbad, CA) in Dulbecco's modified Eagle's medium (containing 110 mg/l pyruvate) supplemented with 10% FBS and incubated (40 min, 37°C, 5% CO₂). Neuron-covered coverslips were loaded with Fura-2 AM (8 μM) in L-15 media containing 20% FBS and incubated (40 min, 37°C). For imaging, the coverslip was placed in a custom-built chamber (bath volume of 600 μl) and superfused at 4 ml/min with Locke solution (34°C) for 15 min before each experiment by an infusion pump.

Changes in intracellular free calcium concentration (intracellular [Ca²⁺]_{free}) were measured by digital microscopy (Universal; Carl Zeiss, Inc., Thornwood, NY) equipped with in-house equipment for ratiometric recording of single cells. The field of cells was monitored by sequential dual excitation, 352 and 380 nm, and the analysis of the image ratios used methods described previously to calculate changes in intracellular [Ca²⁺]_{free} (MacGlashan, 1989). The ratio images were acquired every 6 s. Superfused buffer was stopped 30 s before each drug application, when 300 μl of buffer was removed from the bath and replaced by 300 μl of 2× test agent solution added between image acquisitions. After treatments, neurons were exposed to KCl (30 s, 75 mM) to confirm voltage sensitivity. At the end of experiments, both neurons and HEK 293 cells were exposed to ionomycin (30 s, 1 μM) to obtain a maximal response.

Patch-Clamp Experiments. Conventional whole-cell, patch-clamp recordings were performed at room temperature (21–24°C) using a Multiclamp 700B amplifier and pClamp 9 software (Molecular Devices, Sunnyvale, CA). Pipettes (3–5.5 MΩ) fabricated from borosilicate glass (Sutter Instruments, Novato, CA) were filled with an internal solution composed of 140 mM CsCl, 4 mM MgCl₂, 10 mM HEPES, and 5 mM EGTA; pH was adjusted to 7.2 with CsOH. Coverslips were superfused continuously during recording with an external solution composed of 140 mM NaCl, 2 mM MgCl₂, 5 mM CsCl, 10 mM HEPES, and 10 mM D-Glucose (pH adjusted to 7.4 with NaOH) and gassed with 95% O₂/5% CO₂. Only cells with <10 MΩ series resistances were used and compensated up to 80%. Currents were sampled at 500 Hz, and recordings were filtered at 10 kHz. The membrane potential was held at 0 mV before exposing the cell to a series of voltage ramps (–80 to +80 mV over 500 ms). Data were analyzed using ClampFit software and transferred to Excel spreadsheets or Prism 4 (GraphPad, San Diego, CA) for further analysis.

Chemicals. Stock solutions (200×) of all agonists were dissolved in 100% ethanol and 100% dimethyl sulfoxide for HC-030031. Prostaglandins were purchased from Cayman Chemicals (Ann Arbor, MI). Fura 2AM was purchased from Invitrogen (Carlsbad, CA). 1,2,3,6-Tetrahydro-1,3-dimethyl-N-[4-(1-methylethyl)phenyl]-2,6-[also known as HC-030031 (McNamara et al., 2007)] was purchased from ChemBridge (San Diego, CA). All other chemicals were purchased from Sigma-Aldrich (St. Louis, MO). All drugs were diluted fresh on the day of experiment, except for PGD₂ and PGE₂, which were diluted 5 min before each application to minimize their nonenzymatic dehydration (Ito et al., 1988).

Statistics. For the analysis of Fura-2 AM-loaded cells, the measurement software converted ratiometric information to intracellular [Ca²⁺]_{free} using a default set of Tsien parameters (Gryniewicz et al., 1985) particular to this instrumentation and a broad selection of cells. We did not specifically calibrate the relationship between ratiometric data and absolute calcium concentration, choosing instead to use the default parameters provided and relate all measurements to the peak ionomycin response in each viable cell. This effectively provided the needed cell-to-cell calibration for enumerating individual neuronal responses. Only cells that had a robust response to ionomycin (>400 nM) were included in analyses [maximum HEK 293 cell apparent [Ca²⁺]_{free} response to ionomycin: 1406 nM (standard deviation of 202 nM, 2784 cells); maximum neuronal apparent [Ca²⁺]_{free} response to ionomycin: 1149 nM (standard deviation of 374 nM, 396 cells)]. At each time point for each cell data were presented as the percentage change in intracellular [Ca²⁺]_{free} normalized to ionomycin: response_x = 100 × ([Ca²⁺]_x – [Ca²⁺]_{bi}) / ([Ca²⁺]_{max} – [Ca²⁺]_{bi}), where [Ca²⁺]_x was the apparent [Ca²⁺]_{free} of the cell at a

given time point, $[Ca^{2+}]_{bl}$ was the cell's mean baseline apparent $[Ca^{2+}]_{free}$ measured over 120 s, and $[Ca^{2+}]_{max}$ was the cell's peak apparent $[Ca^{2+}]_{free}$ during ionomycin treatment. For the neuronal experiments, neurons were defined as "responders" to a given compound if the mean response was greater than the mean baseline plus $2 \times$ the S.D. Only neurons that responded to KCl were included in analyses. All data are mean \pm S.E.M. Unpaired *t* tests were used for statistical analysis when appropriate. A *p* value of less than 0.05 was taken as significant.

Results

To test the hypothesis that endogenously occurring prostaglandins containing electrophilic groups might activate TRPA1 on native nociceptive neurons, we used calcium imaging to examine the responses of dissociated mouse trigeminal neurons to the dehydration product of PGD₂, 15-deoxy- $\Delta^{12,14}$ -prostaglandin J₂ (15dPGJ₂, 100 μ M), the TRPA1 agonist AITC (100 μ M), and the TRPV1 agonist capsaicin (1 μ M). All three compounds robustly activated trigeminal neurons, with 50% (81/162) responding to 15dPGJ₂, 49% (388/794) responding to AITC, and 46% (339/730) responding to capsaicin (Fig. 1A, B, and C, respectively). In general, responses to all agonists tended to wane over time, and in some neurons, this happened in the continued presence of the agonist.

Because 15dPGJ₂ possesses electrophilic moieties that may activate TRPA1, and most (86%) trigeminal neurons that responded to 15dPGJ₂ also responded to TRPV1 and/or TRPA1 agonists, we used the selective TRPV1 blocker iodoresiniferatoxin (I-RTX), the nonselective TRP channel blocker ruthenium red (RR), and the selective inhibitor of TRPA1 channel responses HC-030031 (McNamara et al., 2007) to determine whether these agents activated trigeminal neurons through TRP-dependent pathways. I-RTX, at a concentration (1 μ M) that abolished capsaicin sensitivity (0/108 responsive neurons; Fig. 1C), did not reduce the responses of native neurons to 15dPGJ₂ or AITC (Fig. 1, A and B, respectively). By contrast, RR (30 μ M) reduced the response to all three agonists; only 8% (7/86) of neurons responded to 15dPGJ₂, 6% (8/138) responded to AITC, and 9% (5/53) responded to capsaicin (Fig. 1A, B, and C, respectively). In the remaining minority of neurons that retained TRP agonist sensitivity in the presence of RR, the magnitude of their responses was dramatically reduced ($p < 0.005$). HC-030031 (10 μ M) reduced the number of 15dPGJ₂-responsive neurons by 50% and inhibited the response magnitude of these responders by 54% (data not shown). In the presence of 100 μ M HC-030031, only 8% (7/87) of neurons responded to 15dPGJ₂, and the magnitude of the responses of the remaining minority of neurons that retained 15dPGJ₂ sensitivity was dramatically reduced ($p < 0.005$, Fig. 1A). Although the peak mean response to AITC was unaffected by the selective TRPA1 inhibitor, the area under the mean response versus time curve was significantly reduced (by 46%, $p < 0.005$) and the time to peak response was increased from 24 to 120 s in the presence of HC-030031 (Fig. 1B). HC-030031 (100 μ M) did not reduce the response of capsaicin-sensitive native neurons (Fig. 1C).

In further support of the hypothesis that 15dPGJ₂ and AITC share activation pathways in trigeminal neurons, pre-treatment with AITC (100 μ M) for 2 min, followed by a 3-min washout, caused a marked desensitization to subsequent ap-

plication of either AITC (100 μ M) or 15dPGJ₂ (100 μ M), but did not alter the percentage of neurons responding or the maximal response to 1 μ M capsaicin (Fig. 2A and B).

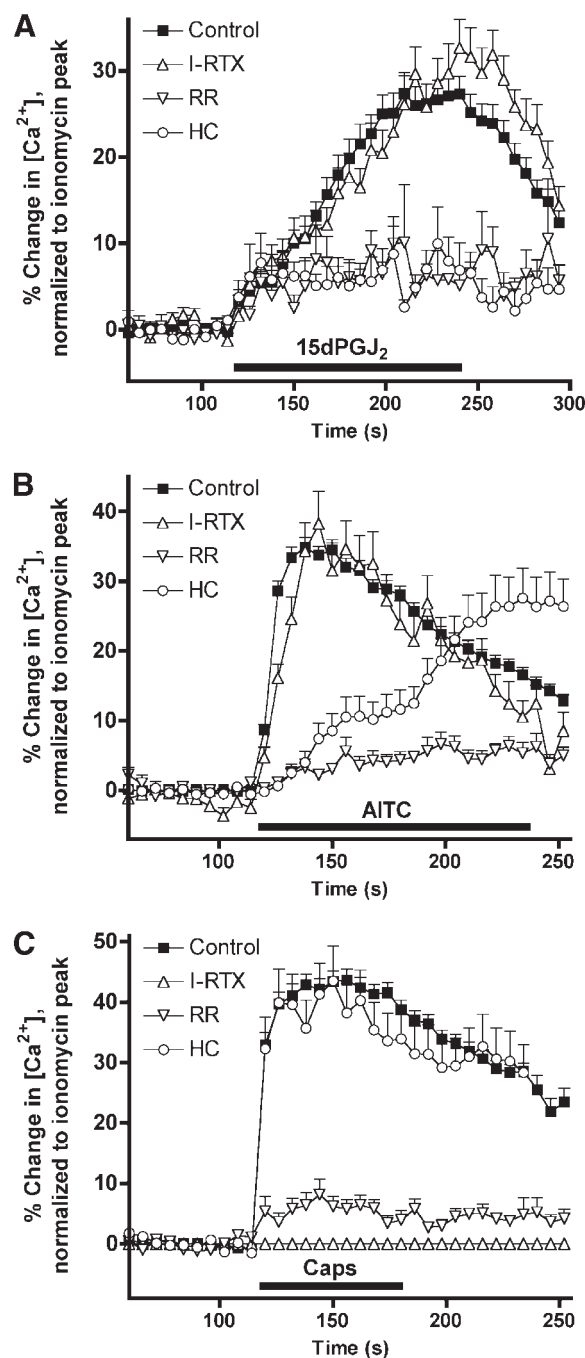


Fig. 1. 15dPGJ₂ mimics the effect of AITC on trigeminal neurons. A, mean \pm S.E.M. Ca^{2+} responses of dissociated trigeminal neurons responding to 15dPGJ₂ (100 μ M) in the presence of vehicle (81 sensitive neurons of 162 tested), the TRPV1 inhibitor iodo-resiniferatoxin (I-RTX, 1 μ M, 59/108), the nonselective TRP inhibitor ruthenium red (RR, 30 μ M, 7/86), or the TRPA1 inhibitor HC-030031 (HC, 100 μ M, 7/87). B, mean \pm S.E.M. Ca^{2+} responses of dissociated trigeminal neurons responding to AITC (100 μ M) in the presence of vehicle (388/794), I-RTX (1 μ M, 37/108), RR (30 μ M, 8/138), or HC (100 μ M, 37/87). C, mean \pm S.E.M. Ca^{2+} responses of dissociated trigeminal neurons responding to capsaicin (Caps, 1 μ M), in the presence of vehicle (339/730), I-RTX (1 μ M, 0/108), RR (30 μ M, 5/53), or HC (100 μ M, 37/87). Blocked line denotes the duration of agonist treatment: 15dPGJ₂ and AITC were applied for 120 s, capsaicin for 60 s. All neurons responded to KCl (75 mM) applied immediately before ionomycin.

To confirm that 15dPGJ₂ activates TRPA1, we examined the response to this agonist in HEK293 cells stably transfected with human TRPA1 (hTRPA1-HEK). As predicted, hTRPA1-HEK cells in calcium imaging assays responded robustly to 100 μM AITC (68 ± 1.5% of ionomycin, *n* = 332), whereas 100 μM AITC failed to activate nontransfected HEK 293 cells (nt-HEK; 0.5 ± 0.1% of ionomycin, *n* = 331). 15dPGJ₂ (1–100 μM) also robustly activated hTRPA1-HEK cells (74 ± 1.7% of ionomycin, *n* = 236), and this response was absent in hTRPA1-HEK cells pretreated with RR (30 μM) (6.4 ± 0.6% of ionomycin, *n* = 241) and in nt-HEK cells (2.4 ± 0.2% of ionomycin, *n* = 317, Fig. 3A-B).

In addition to calcium imaging assays, we performed whole-cell, patch-clamp recordings on hTRPA1-HEK cells, in which, as noted in Materials and Methods, calcium was excluded from the bath and pipette solutions and the chelator EGTA was added to the pipette solution to minimize the impact of calcium-dependent signaling pathways and any confounding direct effects of calcium on channel activity (Doerner et al., 2007; Zurborg et al., 2007). As predicted, AITC activated TRPA1 channels in these cells, with 10 μM

AITC evoking outwardly rectifying currents with peak current densities of -57.4 ± 16.2 pA/pF and 199.6 ± 48.3 pA/pF at -70 and 70 mV, respectively (*n* = 6), in hTRPA1-HEK cells exposed to 500-ms voltage ramps from -80 to $+80$ mV (Fig. 4, A and E). Consistent with our hypothesis that 15dPGJ₂ directly activates TRPA1, voltage ramps in the presence of 10 μM 15dPGJ₂ evoked outwardly rectifying currents (Fig. 4, B and C) of a magnitude (peak current densities of -42.8 ± 10.9 and 131.7 ± 18.5 pA/pF at -70 and 70 mV, respectively; *n* = 8; Fig. 4E) similar to those evoked by the same concentration of AITC. Furthermore, we sought to gauge the selectivity of 15dPGJ₂ in activating nociceptive transducers by applying it to HEK293 cells stably transfected with human TRPV1 channels (hTRPV1-HEK). Using the same voltage ramp protocol that we employed in hTRPA1-HEK cells, we observed small baseline currents with peak densities of -0.8 ± 0.6 and 18.3 ± 6.6 pA/pF at -70 and 70 mV, respectively (*n* = 6), in hTRPV1-HEK cells. Exposing these cells to 10 μM 15dPGJ₂ (*n* = 5) did not appreciably alter baseline currents (peak densities of -0.0 ± 0.5 and 16.3 ± 4.8 pA/pF at -70 and 70 mV, respectively) after ≥ 5 min of treatment (Fig. 4, D and E). By contrast, capsaicin (1 or 3 μM), applied at the end of experiments as a positive control for cell viability and transgene expression,

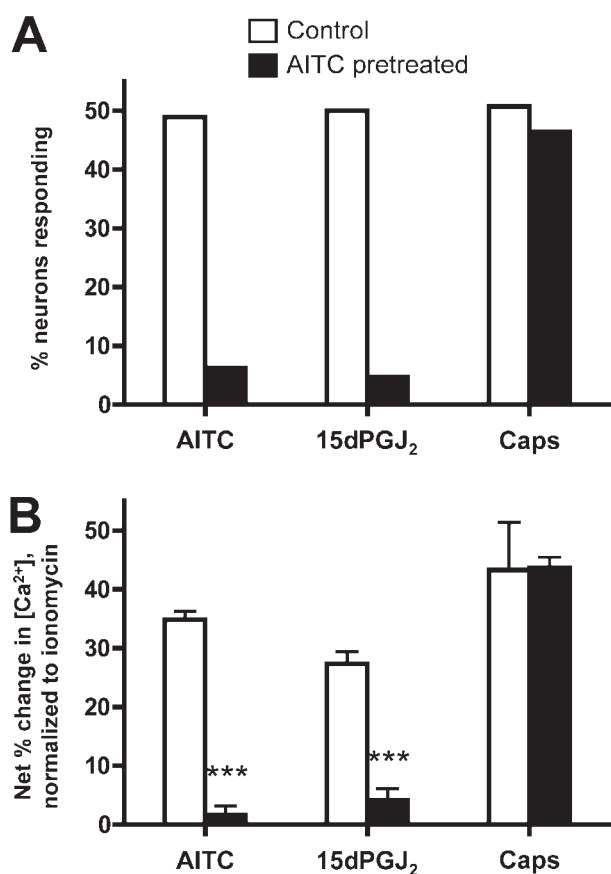


Fig. 2. Responses to 15dPGJ₂ and AITC in trigeminal neurons are inhibited by AITC pretreatment. Ca²⁺ responses to AITC (100 μM), 15dPGJ₂ (100 μM) and capsaicin (Caps, 1 μM) without AITC pretreatment (white columns, data account for 794, 162 and 62 neurons, respectively) or after AITC (100 μM) pretreatment (black columns, data account for 50 neurons). A, percentage of neurons responding to either AITC, 15dPGJ₂ or capsaicin. B, magnitude of the Ca²⁺ responses of neurons that responded to either AITC, 15dPGJ₂, or capsaicin. Data represent the maximum net increase in normalized Ca²⁺ response (during the 120-s drug treatment taken from mean neuron response versus time curves) above the mean response over 120 s before AITC, 15dPGJ₂, or capsaicin treatment (as appropriate) *** Significant decrease in the Ca²⁺ responses after AITC pretreatment (*p* < 0.001).

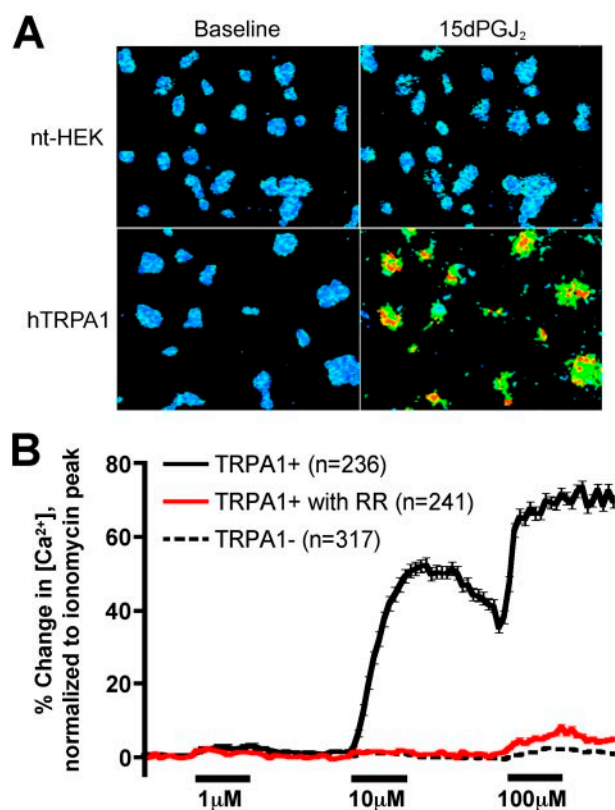


Fig. 3. 15dPGJ₂ activates TRPA1 channels. A, representative Fura 2AM ratiometric image of Ca²⁺ responses of hTRPA1-HEK cells to putative endogenous TRPA1 agonist 15dPGJ₂ (100 μM). B, mean ± S.E.M. Ca²⁺ responses of hTRPA1-HEK cells to putative endogenous TRPA1 agonist 15dPGJ₂ (1, 10 and 100 μM). Legend denotes the number of cells analyzed. 15dPGJ₂ was applied for 60 s (blocked line). Black line denotes responses of hTRPA1-HEK cells, red line denotes responses of hTRPA1-HEK cells in the presence of ruthenium red (RR, 30 μM), and broken line denotes responses of nt-HEK cells.

evoked outwardly rectifying currents with peak densities of -12.2 ± 3.4 and 151.3 ± 33.8 pA/pF at -70 and 70 mV, respectively ($n = 8$; Fig. 4, D and E).

Because some known exogenous activators of TRPA1 (e.g., AITC) and 15dPGJ₂ possess electrophilic moieties, we used calcium imaging to investigate the role of α,β -unsaturated carbonyls in the TRPA1 activation caused by products downstream of COX activity (Fig. 5). Consistent with the hypothesis that electrophilic moieties are required for activation of TRPA1, both PGA₂ (100 μ M), an electrophilic dehydration product of PGE₂, and Δ^{12} -PGJ₂ (100 μ M), an electrophilic intermediate in the metabolism of PGD₂ to 15dPGJ₂, activated hTRPA1-HEK cells but not nt-HEK cells in a manner similar to that of 15dPGJ₂. However, PGD₂ and PGE₂, which do not contain any electrophilic carbons, failed to activate hTRPA1-HEK cells at a concentration of 100 μ M. It is noteworthy that PGB₂ (100 μ M), which is nearly identical in structure to PGA₂, except that its reactive double bond is sterically hindered (Ohno et al., 1990), caused at most a trivial activation of hTRPA1-HEK cells ($4.0 \pm 0.5\%$ of ionomycin). Finally, 100 μ M 8-iso PGA₂, a COX-independent product of oxidative stress-induced peroxidation of arachidonic acid, with an electrophilic group identical to that of PGA₂, also activated hTRPA1-HEK cells but not nt-HEK cells in a manner similar to that of PGA₂. Dose response curves (1, 10, and 100 μ M) were constructed in both hTRPA1-HEK cells and dissociated mouse trigeminal neurons for

those prostanoids that activated the TRPA1 channel (Fig. 5, B and C). Activation of hTRPA1-HEK cells and neurons followed the same rank order: 15dPGJ₂ > Δ^{12} -PGJ₂ > PGA₂ = 8-iso PGA₂, suggesting that these agents increase calcium in neurons through the same mechanism that is activated in hTRPA1-HEK cells.

Discussion

Recent studies have shown that AITC, cinnamaldehyde, and other exogenous irritants with electrophilic groups directly activate TRPA1 (Hinman et al., 2006; Macpherson et al., 2007; McNamara et al., 2007). Our work expands upon these studies by demonstrating that electrophilic molecules that are produced downstream of COX activity during inflammation can also directly activate the channel.

Trigeminal neurons responded to 15dPGJ₂ with an increase in intracellular calcium, and this response was blocked by the nonselective TRP channel blocker ruthenium red and the TRPA1 inhibitor HC-030031, but not by the TRPV1 blocker I-RTX. In addition, AITC selectively desensitized the neurons' response to subsequent exposure to AITC and 15dPGJ₂ but had no effect on subsequent capsaicin-induced responses. Taken together, these results suggest that 15dPGJ₂ activates TRPA1-containing ion channels on trigeminal neurons.

Our observation that 15dPGJ₂, like AITC, causes calcium

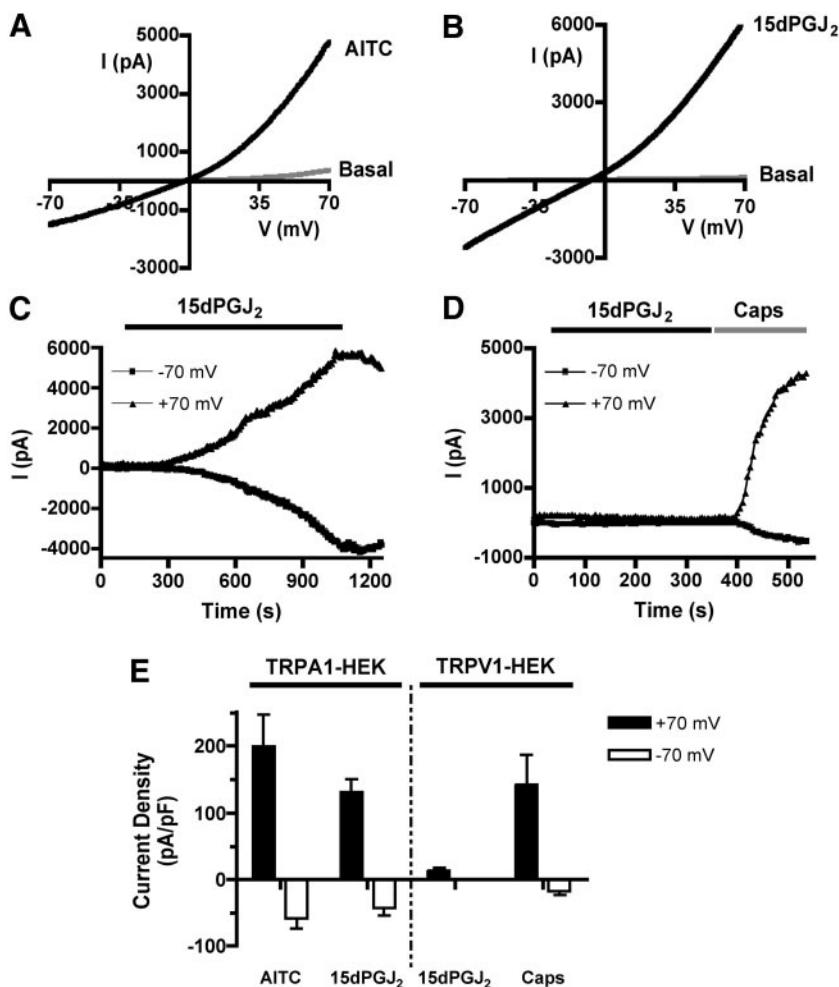


Fig. 4. 15dPGJ₂ evokes currents in TRPA1- but not TRPV1-expressing HEK cells. A, current-voltage relation of AITC (10 μ M)-evoked whole-cell currents in hTRPA1-HEK cells, representative of six separate experiments. B, 15dPGJ₂ (10 μ M) evokes whole-cell currents in hTRPA1-HEK cells similar to AITC, representative of eight separate experiments. Current-voltage traces are represented as the responses to 10 consecutive voltage ramps during basal conditions or after maximum agonist-evoked response had been reached. C, time-course of 15dPGJ₂-evoked currents at -70 and 70 mV in a hTRPA1-HEK cell. D, capsaicin (1 μ M), but not 10 μ M 15dPGJ₂, evokes currents in hTRPV1-HEK cells ($n = 5$). E, mean \pm S.E.M. data demonstrating the effects of 10 μ M 15dPGJ₂ on current densities at -70 and 70 mV in hTRPA1-HEK and hTRPV1-HEK cells relative to the two known channel agonists, AITC and capsaicin, respectively ($n = 5-8$).

influx in hTRPA1-HEK cells but not nt-HEK cells, provides direct evidence that 15dPGJ₂ activates TRPA1. Because TRPA1 can be indirectly stimulated through increases in intracellular calcium (Doerner et al., 2007; Zurborg et al., 2007), it is possible that 15dPGJ₂ activated TRPA1 as a

consequence of uncharacterized mechanism(s) leading to elevated intracellular calcium. This is unlikely, however, because 15dPGJ₂ activated TRPA1 in whole-cell patch-clamp studies carried out at room temperature in the nominal absence of calcium. In addition, our assays detected essentially

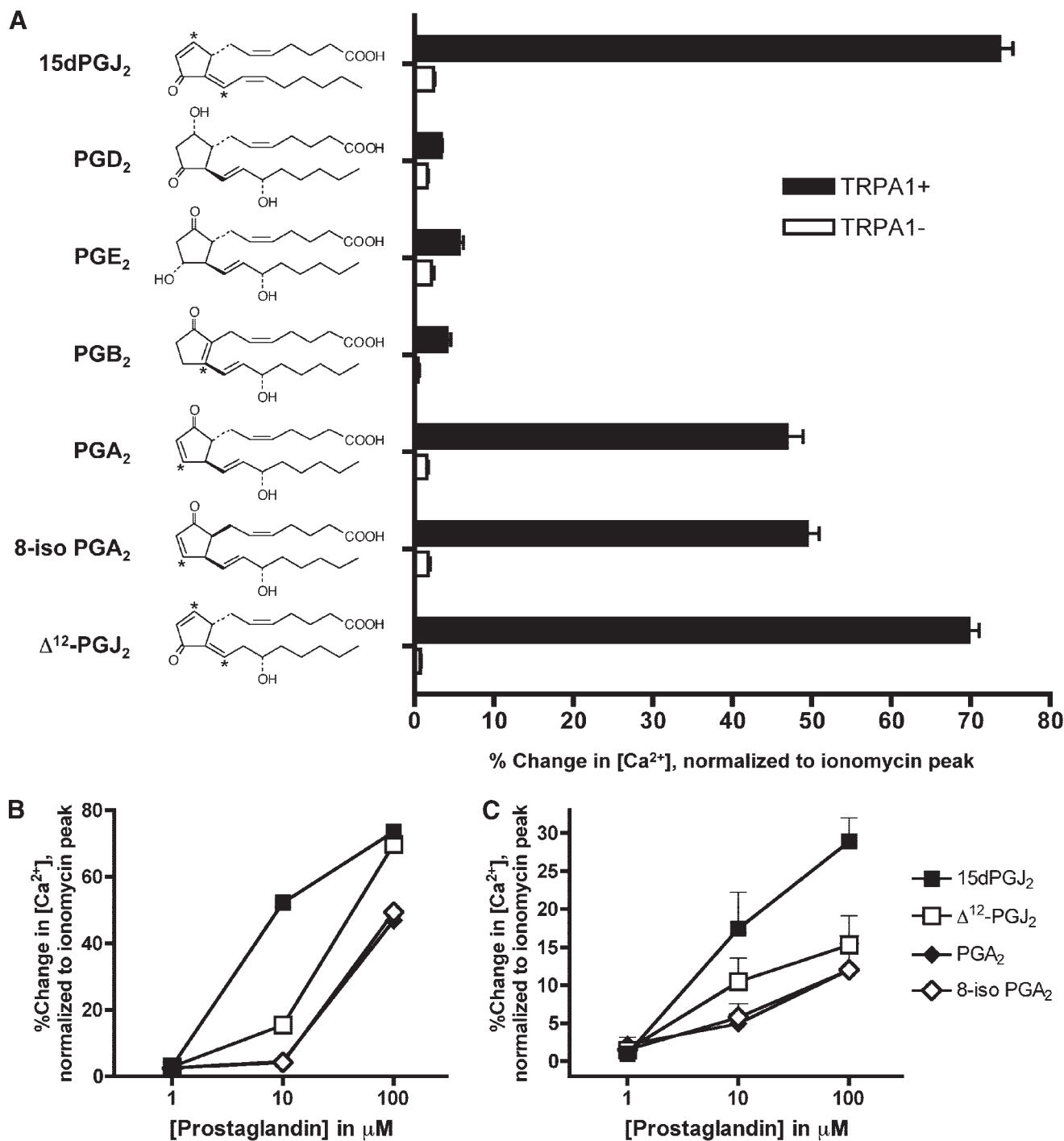


Fig. 5. Electrophilic nature of putative agonists is critical for TRPA1 activity. **A**, maximal Ca²⁺ responses of hTRPA1-HEK and nt-HEK cells to prostanoids (all 100 μM): 15dPGJ₂, PGD₂, PGE₂, PGB₂, PGA₂, 8-iso PGA₂, and Δ¹²-PGJ₂. All hTRPA1-HEK data (black columns) comprise >170 cells; all nt-HEK data (white columns) comprise >240 cells. All drugs were applied for 60 s. Asterisk on prostanoid structures denote reactive carbonyl groups: PGD₂, PGE₂ (lacking group); PGB₂ (sterically hindered group); and 15dPGJ₂, PGA₂, 8-iso PGA₂, and Δ¹²-PGJ₂ (free groups). **B**, dose-response relationships of Ca²⁺ responses of hTRPA1-HEK cells for 15dPGJ₂, Δ¹²-PGJ₂, PGA₂, and 8-iso PGA₂ (1, 10, and 100 μM) (data comprise >170 cells). Data from **A** and **B** represent the maximum response during the 60-s agonist treatment taken from mean cell response versus time curves (with S.E.M. for that data point). **C**, dose-response relationships (1, 10, and 100 μM) of Ca²⁺ responses of prostanoid-sensitive trigeminal neurons for 15dPGJ₂ (69 sensitive neurons of 139), Δ¹²-PGJ₂ (29/136), PGA₂ (13/105), and 8-iso PGA₂ (20/91). Data represent the maximum response during the 120-s drug treatment taken from mean cell response versus time curves (with S.E.M. for that data point). All neurons responded to KCl (75 mM).

no 15dPGJ₂-mediated increase in intracellular calcium in nt-HEK cells.

Prostanoids that contain one or two electrophilic carbons (15dPGJ₂, Δ¹²-PGJ₂, 8-iso PGA₂, and PGA₂) each effectively activated trigeminal neurons and TRPA1-expressing HEK cells with a similar rank order (15dPGJ₂ > Δ¹²-PGJ₂ > 8-iso PGA₂ = PGA₂). By contrast, their structurally related precursors that lack electrophilic carbons (PGD₂, PGE₂) failed to cause more than a trivial activation of TRPA1. It is noteworthy that PGB₂, which is structurally identical to PGA₂ with the exception that its reactive double bond spans the 8 and 12 carbons and is thus sterically hindered, also failed to activate TRPA1. Collectively, these results confirm the absolute requirement of reactive electrophilic moieties for TRPA1 activation by these COX metabolites. Taken together, the findings that 15dPGJ₂ directly activated TRPA1 and that electrophilic carbons were necessary for TRPA1 activation by A- and J-series prostanoids are consistent with the model of TRPA1 activation through direct covalent modification described by Hinman et al. (2006) and Macpherson et al. (2007) for AITC and related irritants.

Prostaglandins such as PGE₂ and PGD₂ are elevated at sites of inflammation (Davies et al., 1984; Woolf and Costigan, 1999) and can be produced by multiple cell types, including nociceptive neurons themselves (Vesin et al., 1995; Chopra et al., 2000), as well as cells such as epithelial cells (Folkerts and Nijkamp, 1998) and mast cells (Roberts et al., 1979), which are commonly found near nerves. While rigorously quantifying the extent to which PGE₂ and PGD₂ are converted into A- and J- series prostaglandins, respectively, is challenging because of their reactivity, micromolar levels of 15dPGJ₂ have been detected in inflammatory exudates in a rat pleurisy model (Gilroy et al., 1999) and in lymph nodes of mice displaying delayed type hypersensitivity reactions in response to methylated bovine serum albumin sensitization and challenge (Trivedi et al., 2006). These levels were dramatically decreased by treatment with the COX-2 inhibitor NS398 (Gilroy et al., 1999) or targeted deletion of hematopoietic PGD₂ synthase (Trivedi et al., 2006). Finally, there is at least preliminary evidence that production of A- and J-series prostanoids may also occur in humans (Chen et al., 1999; Blanco et al., 2005).

Unlike the other prostanoids tested in this study, which require COX activity for their production, the isoprostane 8-iso PGA₂ is produced nonenzymatically through oxidative metabolism of membrane phospholipids (Roberts and Morrow, 2002). Thus, 8-iso PGA₂ activates TRPA1, mimicking the activation that we and others have described previously for 4-hydroxynonenal (Taylor-Clark et al., 2007; Trevisani et al., 2007), another product of oxidative metabolism of membrane phospholipids. Thus, these data suggest that a variety of reactive electrophiles produced downstream of COX activation and/or lipid peroxidation may contribute to nociception by directly activating TRPA1 at local sites of inflammation.

In summary, we demonstrate evidence of a novel mechanism through which a subset of reactive metabolites of PGD₂ and PGE₂ may stimulate nociceptive neurons through direct activation of TRPA1.

Acknowledgments

We thank David Bettoun and Mike McQueney for insightful discussions regarding the chemistry of reactive electrophiles and Natalie Tighe for providing stably transfected hTRPA1-HEK cells.

References

- Bandell M, Story GM, Hwang SW, Viswanath V, Eid SR, Petrus MJ, Earley TJ, and Patapoutian A (2004) Noxious cold ion channel TRPA1 is activated by pungent compounds and bradykinin. *Neuron* **41**:849–857.
- Bautista DM, Jordt SE, Nikai T, Tsuruda PR, Read AJ, Poblete J, Yamoah EN, Basbaum AI, and Julius D (2006) TRPA1 mediates the inflammatory actions of environmental irritants and proalgesic agents. *Cell* **124**:1269–1282.
- Blanco M, Moro MA, Davalos A, Leira R, Castellanos M, Serena J, Vivancos J, Rodriguez-Yanez M, Lizasoain I, and Castillo J (2005) Increased plasma levels of 15-deoxyDelta prostaglandin J₂ are associated with good outcome in acute atherothrombotic ischemic stroke. *Stroke* **36**:1189–1194.
- Burian M and Geisslinger G (2005) COX-dependent mechanisms involved in the antinociceptive action of NSAIDs at central and peripheral sites. *Pharmacol Ther* **107**:139–154.
- Chen Y, Morrow JD, and Roberts LJ 2nd (1999) Formation of reactive cyclopentenone compounds in vivo as products of the isoprostane pathway. *J Biol Chem* **274**:10863–10868.
- Chopra B, Giblett S, Little JG, Donaldson LF, Tate S, Evans RJ, and Grubb BD (2000) Cyclooxygenase-1 is a marker for a subpopulation of putative nociceptive neurons in rat dorsal root ganglia. *Eur J Neurosci* **12**:911–920.
- Davies P, Bailey PJ, Goldenberg MM, and Ford-Hutchinson AW (1984) The role of arachidonic acid oxygenation products in pain and inflammation. *Annu Rev Immunol* **2**:335–357.
- Doerner JF, Gisselmann G, Hatt H, and Wetzel CH (2007) Transient receptor potential channel A1 is directly gated by calcium ions. *J Biol Chem* **282**:13180–13189.
- Fitzpatrick FA and Waynald MA (1981) Albumin-lipid interactions: prostaglandin stability as a probe for characterizing binding sites on vertebrate albumins. *Biochemistry* **20**:6129–6134.
- Folkerts G and Nijkamp FP (1998) Airway epithelium: more than just a barrier! *Trends Pharmacol Sci* **19**:334–341.
- Gayarre J, Sanchez D, Sanchez-Gomez FJ, Terron MC, Llorca O, and Perez-Sala D (2006) Addition of electrophilic lipids to actin alters filament structure. *Biochem Biophys Res Commun* **349**:1387–1393.
- Gilroy DW, Colville-Nash PR, Willis D, Chivers J, Paul-Clark MJ, and Willoughby DA (1999) Inducible cyclooxygenase may have anti-inflammatory properties. *Nat Med* **5**:698–701.
- Grynkiwicz G, Poenie M, and Tsien RY (1985) A new generation of Ca²⁺ indicators with greatly improved fluorescence properties. *J Biol Chem* **260**:3440–3450.
- Hayes P, Meadows HJ, Gunthorpe MJ, Harries MH, Duckworth DM, Cairns W, Harrison DC, Clarke CE, Ellington K, Prinjha RK, et al. (2000) Cloning and functional expression of a human orthologue of rat vanilloid receptor-1. *Pain* **88**:205–215.
- Herlong JL and Scott TR (2006) Positioning prostanoids of the D and J series in the immunopathogenic scheme. *Immunol Lett* **102**:121–131.
- Hill K and Schaefer M (2007) TRPA1 is differentially modulated by the amphipathic molecules trinitrophenol and chlorpromazine. *J Biol Chem* **282**:7145–7153.
- Hinman A, Chuang HH, Bautista DM, and Julius D (2006) TRP channel activation by reversible covalent modification. *Proc Natl Acad Sci U S A* **103**:19564–19568.
- Hjerling-Leffler J, Alqatari M, Ernfors P, and Koltzenburg M (2007) Emergence of functional sensory subtypes as defined by transient receptor potential channel expression. *J Neurosci* **27**:2435–2443.
- Ito S, Tanaka T, Hayashi H, and Hayaishi O (1988) Problems in production of prostaglandin D₂-specific antibody. *Eicosanoids* **1**:111–116.
- Jenkins DW, Feniuk W, and Humphrey PP (2001) Characterization of the prostanoid receptor types involved in mediating calcitonin gene-related peptide release from cultured rat trigeminal neurons. *Br J Pharmacol* **134**:1296–1302.
- Jordt SE, Bautista DM, Chuang HH, McKemy DD, Zymunt PM, Hogestatt ED, Meng ID, and Julius D (2004) Mustard oils and cannabinoids excite sensory nerve fibres through the TRP channel ANKTM1. *Nature* **427**:260–265.
- Katsura H, Tsuzuki K, Noguchi K, and Sakagami M (2006) Differential expression of capsaicin-, menthol-, and mustard oil-sensitive receptors in naive rat geniculate ganglion neurons. *Chem Senses* **31**:681–688.
- Kwan KY, Allchorne AJ, Vollrath MA, Christensen AP, Zhang DS, Woolf CJ, and Corey DP (2006) TRPA1 contributes to cold, mechanical, and chemical nociception but is not essential for hair-cell transduction. *Neuron* **50**:277–289.
- MacGlashan D Jr (1989) Single-cell analysis of Ca⁺⁺ changes in human lung mast cells: graded vs. all-or-nothing elevations after IgE-mediated stimulation. *J Cell Biol* **109**:123–134.
- Macpherson LJ, Dubin AE, Evans MJ, Marr F, Schultz PG, Cravatt BF, and Patapoutian A (2007) Noxious compounds activate TRPA1 ion channels through covalent modification of cysteines. *Nature* **445**:541–545.
- McNamara CR, Mandel-Brehm J, Bautista DM, Siemens J, Deranian KL, Zhao M, Hayward NJ, Chong JA, Julius D, Moran MM, et al. (2007) TRPA1 mediates formalin-induced pain. *Proc Natl Acad Sci U S A* **104**:13525–13530.
- Moriyama T, Higashi T, Togashi K, Iida T, Segi E, Sugimoto Y, Tominaga T, Narumiya S, and Tominaga M (2005) Sensitization of TRPV1 by EP1 and IP1 reveals peripheral nociceptive mechanism of prostaglandins. *Mol Pain* **1**:3.
- Ohno K, Higaki J, Takechi S, and Hirata M (1990) Specific role of an alpha, beta-unsaturated carbonyl group in gamma-glutamylcysteine synthetase induction by prostaglandin A₂. *Chem Biol Interact* **76**:77–87.
- Roberts LJ, 2nd, Lewis RA, Oates JA, and Austen KF (1979) Prostaglandin throm-

- boxane, and 12-hydroxy-5,8,10,14-eicosatetraenoic acid production by ionophore-stimulated rat serosal mast cells. *Biochim Biophys Acta* **575**:185–192.
- Roberts LJ, 2nd and Morrow JD (2002) Products of the isoprostane pathway: unique bioactive compounds and markers of lipid peroxidation. *Cell Mol Life Sci* **59**:808–820.
- Stamatakis K and Perez-Sala D (2006) Prostanoids with cyclopentenone structure as tools for the characterization of electrophilic lipid-protein interactomes. *Ann N Y Acad Sci* **1091**:548–570.
- Story GM, Peier AM, Reeve AJ, Eid SR, Mosbacher J, Hricik TR, Earley TJ, Hergarden AC, Andersson DA, Hwang SW, et al. (2003) ANKTM1, a TRP-like channel expressed in nociceptive neurons, is activated by cold temperatures. *Cell* **112**:819–829.
- Taylor-Clark TE, Kollarik M, MacGlashan DW, Jr. and Undem BJ (2005) Nasal sensory nerve populations responding to histamine and capsaicin. *J Allergy Clin Immunol* **116**:1282–1288.
- Taylor-Clark TE, Undem BJ, and McAlexander MA (2008) 4-Hydroxynonenal: a potential endogenous activator of transient receptor potential A1 (TRPA1) channels (Abstract). *Am J Respir Crit Care Med* **175**:A667.
- Trevisani M, Siemens J, Materazzi S, Bautista DM, Nassini R, Campi B, Imamachi N, Andre E, Patacchini R, Cottrell GS, et al. (2007) 4-Hydroxynonenal, an endogenous aldehyde, causes pain and neurogenic inflammation through activation of the irritant receptor TRPA1. *Proc Natl Acad Sci U S A* **104**:13519–13524.
- Trivedi SG, Newson J, Rajakariar R, Jacques TS, Hannon R, Kanaoka Y, Eguchi N, Colville-Nash P, and Gilroy DW (2006) Essential role for hematopoietic prostaglandin D2 synthase in the control of delayed type hypersensitivity. *Proc Natl Acad Sci U S A* **103**:5179–5184.
- Vesin MF, Urade Y, Hayaishi O, and Droz B (1995) Neuronal and glial prostaglandin D synthase isozymes in chick dorsal root ganglia: a light and electron microscopic immunocytochemical study. *J Neurosci* **15**:470–476.
- Woolf CJ and Costigan M (1999) Transcriptional and posttranslational plasticity and the generation of inflammatory pain. *Proc Natl Acad Sci U S A* **96**:7723–7730.
- Xu H, Delling M, Jun JC, and Clapham DE (2006) Oregano, thyme and clove-derived flavors and skin sensitizers activate specific TRP channels. *Nat Neurosci* **9**:628–635.
- Zurborg S, Yurgionas B, Jira JA, Caspani O, and Heppenstall PA (2007) Direct activation of the ion channel TRPA1 by Ca²⁺. *Nat Neurosci* **10**:277–279.

Address correspondence to: Dr. Bradley J. Undem, Johns Hopkins Medical Institutions, Johns Hopkins Asthma and Allergy Center, 3A.44, Baltimore, MD 21224. E-mail: bundem@jhmi.edu
